Real-time Post-earthquake Assessment of Civil Structures in the Presence of after-shocks

F. Jalayer, D. Asprone, A. Prota & G. Manfredi
Department of Structural Engineering, University of Naples Federico II, Naples, Italy

Keywords: seismic reliability, after-shock hazard, post-earthquake assessment, after-shock sequence, life safety

Abstract

The post-earthquake assessment of existing structures can be further complicated by the progressive damage induced by the occurrence of a sequence of after-shocks. This work presents a simple method for the calculation of the probability of exceeding a certain limit state in a given interval of time. The time-decaying mean daily rate of occurrence of significant after-shock events is modeled by employing a generic after-shock model. The occurrence of after-shock events is modeled using a non-homogenous Poisson model. An equivalent single-degree of freedom structure is used in order to evaluate the progressive damage caused by a sequence of after-shock events. Given the time history of the main-shock and the residual damage caused by it, the probability of exceeding a set of discrete limit states in a given interval of time is calculated. Of particular importance is the time-variant probability of exceeding the limit state in a 24-hour (a day) interval of time which can be used as a proxy for the life-safety considerations regarding the re-occupancy of the structure. The method presented herein can also be used in an adaptive manner, conditioning progressively on the time-histories of after-shock events following the main-shock and the corresponding residual damage caused by them.

1 INTRODUCTION

The inspection and management of the civil structures, after the occurrence of a severe earthquake event is subjected to considerable challenges. The post-earthquake deterioration as a result of the sequence of after-shocks threaten significantly eventual inspection and/or re-occupancy of these structures. In fact, a significant main-shock is often followed by a number of after-shock events (usually smaller in moment magnitude) which take place in a limited area (i.e., the after-shock zone) around the epicenter of the main event. This sequence of after-shock events can last in some cases for months. Although these events are smaller in magnitude with respect to the main event, they can prove to be destructive on the structure. This is due to both the significant number of after-shocks (in some cases up to 6000) and also due to the fact that the structure has probably already suffered damage from the main event.

The occurrence of main-shock events is often modeled by a homogenous Poisson stochastic process with time-invariant rate. However, the sequence of after-shocks are characterized by a rate of occurrence that decreases as a function of time elapsed after the earthquake. Therefore, the occurrence of the after-shocks are modeled by a non-homogenous Poisson process with a decreasing time-variant rate. The first few days after the occurrence of main-shock can be very decisive as there is urgent need for re-entrance in the building (for rescue or for inspection) while the mean daily after-shock rate is quite considerable.

The after-shock assessment of civil structures can be considered as decision making between a set of actions such as, to evacuate, to enter for inspection operations, to re-occupy the structure, etc. In the context of performance-based design, several performance objectives (e.g., ensuring life-safety in case of extreme and rare events) can be considered for a set of (discrete) limit states. Yeo and Cornell (Yeo and Cornell, 2008) have proposed a decision-making framework based on stochastic dynamic programming which minimizes the expected life-cycle cost subjected to acceptable life-safety constraints. As a proxy for life-safety, they have employed an equivalent constant collapse rate for the main-shock damaged structure (Yeo and Cornell, 2008b).

The present study presents a procedure for calculating the time-dependent *probability* of exceeding the limit states corresponding to various discrete performance objectives. A simple deteriorating single degree of freedom (SDOF) model of the structure is used in order to study the damages induced as a result of a sequence of after-shocks. As a criteria for assessment of the decisions regarding re-entrance for inspections purposes, the (time-dependent) probability of exceeding the limit state of life-safety in a 24-hour interval is compared to an acceptable threshold. The less severe limit states of severe damage and onset of damage can be used in a similar manner in order to make decisions regarding the re-occupancy and serviceability of the structure.

2 METHODOLOGY

The objective of this methodology is to calculate the time-dependent probability of exceeding various discrete limit states in a given interval of time for a given structure subjected to a sequence of after-shocks. The methodology presented herein for the evaluation of the limit state probability in a given time interval can be used for decision making between different viable actions such as, re-entry/evacuation, re-occupancy/shutting down. This methodology starts from the state of the structure after it is hit by a main-shock. Therefore, given that the main shock wave-forms are available, the damages undergone by the structural model can be evaluated. Since the clustering of earthquakes usually occurs near the location of the main-shock also referred to as the *after-shock zone*, it is assumed that the source-to-cite distance is constant for the sequence of earthquakes including the main-shock and after-shocks events. An important characteristic of the sequence of after-shocks following the main-shock is that the rate of after-shocks dies off quickly with time elapsed since the main-shock. In the absence of specific time-decaying laws regarding a particular after-shock sequence, a generic after-shock model can be employed. The methodology presented is of an adaptive nature; that is, with occurrence of more after-shock events, the state of the structure can be updated by evaluating the damages undergone by the structural model subjected to the sequence of main-shock and after-shocks.

2.1 *The probabilistic seismic after-shock hazard*

The probability that the structural acceleration at the fundamental period of the structure S_a exceeds a given level x given that a significant after-shock event with a constant source-to-site distance R has taken place denoted by $P(S_a > x|\mathrm{as})$ can be calculated as:

$$P(S_a > x|\mathrm{as}) = \int_{M_l}^{M_m} P(S_a > x|m, R)p(m)dm \tag{1}$$

where M_m is the moment-magnitude for the main-shock event and M_l is the lower-bound for the moment magnitude for the earthquake events of engineering interest. The term $P(S_a > x|m, R)$ can be calculated using the parameters of the ground motion prediction relation for the site and $p(m)$ is the truncated Gutenberg-Richter probability density function for moment magnitude:

$$p(m) = \frac{\beta \cdot e^{-\beta \cdot m}}{e^{-\beta \cdot M_l} - e^{-\beta \cdot M_m}} \tag{2}$$

$\beta = b \log 10$ where b is related to the seismicity of the site. The mean daily rate of exceeding a given spectral acceleration level can be calculated by multiplying Equation 1 by the average daily rate of occurrence of after-shock events:

$$H(S_a > x) = \nu(t) \cdot P(S_a > x|\text{as}) \tag{3}$$

where $\nu(t)$ is the time-dependent average daily rate of occurrence of after-shocks after t days are elapsed from the main-shock.

2.1.1 *Updating the hazard after the occurrence of the main-shock*

After the occurrence of a main-shock, assuming that its wave-form is known, the probability of exceeding a given value of spectral acceleration in Equation 1 can be updated using the Bayes formula taking into account the spectral acceleration at the fundamental period of the structure for the main-shock, $S_{a,ms}$:

$$\begin{aligned} p(S_{a,as} = x|S_{a,ms}, \text{as}) = \\ = \frac{p(S_{a,ms}|S_{a,as} = x, \text{as})p(S_{a,as} = x|\text{as})}{\sum_x p(S_{a,ms}|S_{a,as} = x, \text{as})p(S_{a,as} = x|\text{as})} \end{aligned} \tag{4}$$

where $p(S_{a,as} = x|S_{a,ms}, \text{as})$ denotes the probability density function (PDF) for the spectral acceleration of the after-shock given that the spectral acceleration of the main-shock is known, $p(S_{a,ms}|S_{a,as} = x, \text{as})$ is the probability density function for main-shock given the after-shock spectral acceleration is known and $p(S_{a,ms}|S_{a,as} = x, \text{as})$ is the PDF for after-shock spectral acceleration before having the extra information. Having calculated the updated PDF, the updated probability of exceeding a given after-shock spectral acceleration can be calculated using the following relationship:

$$P(S_a = x) = -\frac{P(S_a > x)}{dx} \tag{5}$$

2.2 *The assessment of time-dependent limit state probability*

Let T_{max} denote a given interval of time elapsed after a main-shock has taken place, N the maximum number of after-shock events that can take place during T_{max} * and τ the repair time for the structure. The probability $P(LS; T_{max})$ of exceeding a specified limit state LS in time T_{max} can be written as:

$$P(LS; T_{max}) = \sum_{i=1}^{N} P(LS|i)P(i; T_{max}) \tag{6}$$

Where $P(LS|i)$ is the probability of exceeding the limit state given that exactly i after-shocks take place in time T_{max} and $P(i; T_{max})$ is the probability that exactly i after-shock events take place in time T_{max}. It is assumed that the after-shock hazard for the site of the structure is expressed by a non-homogenous *Poisson* probability distribution with the time-decaying rate denoted by $\nu(t)$. The probability of having exactly i events in time T_{max} can be calculated as:

$$P(i; T_{max}) = \frac{(\int_0^{T_{max}} \nu(t)dt)^i e^{-\int_0^{T_{max}} \nu(t)dt}}{i!} \tag{7}$$

The term $P(LS|i)$ can be calculated by taking into account the set of mutually exclusive and collectively exhaustive (MECE) events that the limit state is exceeded at one and just one of the previous after-shock events:

$$\begin{aligned} P(LS|i) = P(C_1 + \overline{C_1}C_2 + \cdots + \\ + \overline{C_1 C_2 \cdots C_{i-1}} C_i|i) \end{aligned} \tag{8}$$

where $C_j, j = 1 : i$ indicates the event of exceeding the limit state LS due to the jth event and $\overline{C_j}$ indicates the negation of C_j. The probability $P(C_j|i)$ can be further broken down into the sum of the probabilities of two MECE events that event j hits the "intact" structure (i.e., damaged only by the main-shock) and that the event j hits the damaged structure:

$$P(C_j|i) = P(C_j I|i) + P(C_j D|i) \tag{9}$$

*The number of possible events N in time T_{max} is unbounded.

Equation 9 can be further expanded as follows:

$$P(C_j|i) = P(C_j|I,i)P(I|i) + \\ + \sum_{k=1}^{j-1} P(C_j|k,i)P(k|i) \tag{10}$$

where $\{k : k = 1, 2, \cdots, i-1\}$ indicates the number of times the structure has been damaged by an after-shock before reaching the target limit state, implying that the structure deteriorates with the occurrence of each event. The formulation in Equation 10 is based on the consideration that an event can hit a structure already damaged by one or more *previous* event(s). This situation occurs only if the inter-arrival time IAT for events is smaller than the repair time τ. Moreover, since the inter-arrival time can be described by the *Exponential* probability distribution, the probability that the IAT is less than or equal to the repair time τ can be expressed as $1 - \exp(-\int_0^\tau \nu(t)dt)$ times the probability $\exp(-\int_0^\tau \nu(t)dt)$ that the structure is intact before k after-shock events. Therefore, the probability that the structure is damaged k times before reaching LS is equal to:

$$P(k|i) = e^{-\int_0^\tau \nu(t)dt}(1 - e^{-\int_0^\tau \nu(t)dt})^k \tag{11}$$

Assuming that the structure under repair is hit by another after-shock event, the repair operations are going to resume from zero. Thus, the probability that the structure is intact when hit by an event can be calculated as the probability that the IAT is greater than the repair time:

$$P(I|i) = e^{-\int_0^\tau \nu(t)dt} \tag{12}$$

Observing Equation 10, one can identify the sequence of the limit state probability terms terms, namely, $P(C_j|I,i)$ and $P(C_j|k,i)$ where $k = 1, \cdots, (j-1)$.

2.2.1 *Estimation of limit state probabilities*

In order to calculate the sequence of limit state probability terms $P(C_j|D_k,i)$ where $k = 1, \cdots, (j-1)$, the following procedure is applied. A selection of n earthquake records (consisted of main-shocks and after-shocks) is selected. In order to emulate the deterioration caused by the sequence of after-shocks, each ground motion is applied k times in sequence to the structural model. The maximum displacement response of the structure due to the sequence of k events denoted by $Y(k)$ is related to the spectral acceleration at the fundamental period of the structure denoted by S_a using the linear least squares (in the logarithmic scale). That is, the median for maximum displacement is described by $\eta_{Y|S_a}(k) = a \cdot S_a^b$ and that the standard deviation (of the logarithm) of $Y(k)$ given S_a is calculated as:

$$\sigma_{\ln Y(k)|S_a} = \sqrt{\frac{\sum_1^n (\ln Y(k) - \ln a \cdot S_a^b)^2}{n-2}} \tag{13}$$

where a and b are regression coefficients calculated as:

$$a = \frac{\sum \log Y_i \sum \log S_{a,i}^2 - \sum \log S_{a,i} \sum \log Y_i \log S_{a,i}}{n \sum \log S_{a,i}^2 - (\sum \log S_{a,i})^2}$$

$$b = \frac{n \sum \log Y_i \log S_{a,i} - \sum \log S_{a,i} \sum \log Y_i}{n \sum \log S_{a,i}^2 - (\sum \log S_{a,i})^2} \tag{14}$$

The limit state probability $P(C_j|D_k,i,S_a)$ can be calculated as:

$$P(C_j|D_k,i,S_a) = 1 - \Phi\left(\frac{\log Y_{C_j} - \log(\eta_{Y|S_a}(k))}{\sigma_{\ln Y(k)|S_a}}\right) \tag{15}$$

In order to calculate $P(C_j|D_k,i)$, the expression in Equation 15 needs to be integrated with the probability density function (pdf) for the spectral acceleration given that a significant after-shock has taken place, calculated by the differentiation of the complementary cumulative distribution function for spectral acceleration given a significant after-shock has taken place in Equation 3. Therefore:

$$P(C_j|D_k,i) = \int_0^\infty P(C_j|D_k,i,S_a) \cdot p(Sa|\text{as}) \tag{16}$$

The procedure described in this section for the calculation of the probability of exceeding limit state LS can be employed to calculate the limit state probabilities for an increasing sequence of limit states, e.g., from serviceability to collapse.

2.3 *The probability of collapse in a 24-hour interval*

In the previous section, it is explained how the probability of exceeding the limit state LS in a given interval of time T_{max} can be calculated from Equation 6. However, it is of interest to calculate the probability of exceeding the limit state in a reference time interval(e.g., 24 hours). The probability of exceeding the limit state in the reference time interval $[T, T + \Delta T]$ can be calculated as:

$$P(LS; [T, T+\Delta T]) = P(LS; T+\Delta T) - P(LS; T) \quad (17)$$

Therefore, the probability of exceeding the limit state in one day can be calculated from Equation 17, by setting ΔT equal to one.

3 NUMERICAL EXAMPLE

The methodology presented in the previous section is applied to an existing structure as a case study.

3.1 *Structural model*

The case-study building is a generic five-story RC frame structure. The structural model is illustrated in Figure 1, presenting a plan of the generic storey. Each storey is 3.00m high, except the second one, which is 4.00m high. The non-linear behavior in the sections is modeled based on the concentrated plasticity concept. It is assumed that the plastic moment in the hinge sections is equal to the ultimate moment capacity in the sections which is calculated using the Mander (Mander et al., 1988) model for concrete and elastic-plastic model for steel rebar. In order to simplify the structural analyses, an equivalent degrading (SDOF) system is used as the structural model. In order to model the the non-linear characteristics of the equivalent SDOF system, a non-linear static analysis on the case-study structure is performed. The resulting pushover curve is transformed into that of an equivalent SDOF system based on the first mode shape of the structure. Based on the resulting equivalent pushover curve, the non-linear degrading hysteresis model for the equivalent SDOF system is constructed. More details can be found in a previous work by the authors (Asprone et al. 2008).

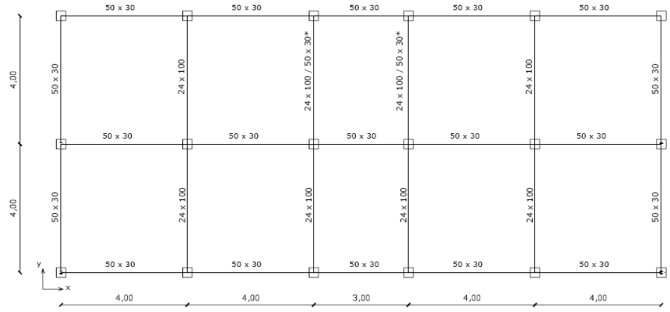

Figure 1: Storey view (dimensions in m) *Beam frame labels indicate the section dimensions in cm; column sections are all (30×30) *this frame represents both storey beams (24×100) and stair knee beams (50×30)*

3.2 *Probabilistic seismic after-shock hazard assessment*

It is assumed that the generic structure is located in central Italy. The after-shock hazard at the site is calculated assuming the main-shock and after-shocks all take place at a constant source-to-site distance of 10km. The average daily rate of occurrence of after-shock events with magnitude between M_l and M_m is calculated from a generic after-shock sequence (Reasenberg and Jones, 1989) as follows:

$$\nu(t) = \frac{10^{a+b(M_m-M_l)} - 10^a}{(t+c)^p} \quad (18)$$

where $a = -1.67$, $b = 0.91$, $M_m = 6.3$, $M_l = 4.7$, $c = 0.05$ and $p = 1.08$. The probability of exceeding a given value of spectral acceleration given an after-shock event has occurred is calculated from Equation 1 using the ground motion prediction relationship by Sabetta and Pugliese (Sabetta and Pugliese, 1996) for the horizontal component of the ground motion on rock (type A) and plotted in Figure 2. The site of the structure is assumed to be situated in the zone number 920 of the seismogenetic hazard zonation (ZS9, (Meletti and Valensise, 2004)). In order to update the aftershock hazard given that the main-shock wave-form is known, a set of main-shocks and the corresponding after-

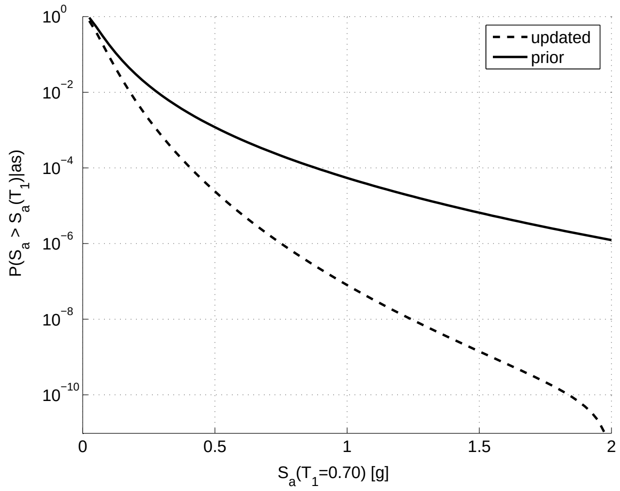

Figure 2: The probability of exceeding a given level of S_a given the occurrence of an after-shock

shocks (registered at the same station) are gathered from European strong motion database (*http://www.isesd.cv.ic.ac.uk/ESD/*) and their spectral acceleration values at the fundamental period of the structure are calculated. The resulting data-points together with the parameters of a linear least squares performed on after-shock spectral acceleration (as the dependent variable) versus the corresponding main-shock spectral acceleration (as the independent variable) are plotted in Figure 3. The regression results can be used to calculate the term $p(S_{a,ms}|S_{a,as} = x, \text{as})$ assuming that $S_{a,ms} = 0.3g$. The probability of exceeding the spectral acceleration taking into account the specific main-shock information is updated using Equations 4 and 5. The resulting updated probability of exceeding a given after-shock spectral acceleration is plotted in Figure 2. It can be observed that the additional information about the main-shock reduces significantly the aftershock hazard.

3.3 *Calculation of failure probabilities*

In order to calculate the failure probabilities due to the sequence of after-shock events, a set of 50 ground motion records (consisting of main-shocks and after-shocks) are chosen. Each ground motion record is applied sequentially k times on the equivalent SDOF model. The probability of failure given that a sequence of k after-shocks has occurred is calculated following the procedure ex-

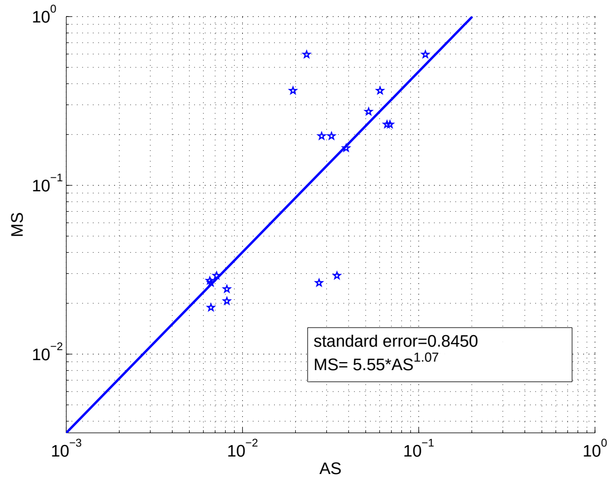

Figure 3: Predicting $S_a(T_1)$ of the main-shock given the $S_a(T_1)$ of the after-shock using linear least squares in the logarithmic scale

plained in section 2.2.1.

3.4 *Time-dependent limit-state probability*

The performance objectives for post-earthquake assessment of the case-study structure are defined in terms of discrete limit states of, serviceability, onset of damage, severe damage and collapse. These limit states have been defined in relation to the maximum roof displacement. Table 1 illustrates the limit states and their corresponding engineering demand parameter threshold. The limit

Table 1: Equivalent SDOF maximum displacement [meters]

LS	Maximum Roof Displacement
Serviceability	0.01
Onset of damage	0.02
Severe Damage	0.06
Collapse	0.10

states are distinguished in terms of increasing levels of the maximum displacement for the equivalent SDOF system. A ground motion record with moment magnitude equal to 6.3 is assumed to be the main shock event and is applied to the equivalent SDOF system. Two distinct cases are studied, the residual displacement of the SDOF system is calculated to be equal to (1) 0.015m (*low-residual* case, 15% of the total displacement capacity) and (2) 0.05m (the *high-residual* case, 50% of the displacement capacity). In first case, the structure has exceeded the limit state of serviceability due to the main-shock and in the second case the structure is very close to the onset of severe damage. Assuming that in time T_{max} a maximum of 20 significant after-shock events (i.e., $M_l > 4.7$ for zone 920 can take place), the sequence of structural limit state probabilities due to the occurrence of the after-shocks is calculated by following the procedure discussed in section 2.2.1. The limit state probabilities $P(C_j|D_k, i)$ for $k = i = 1 : 20$ are plotted in Figure 4 where the solid lines correspond to the low-residual case and the dashed lines correspond to the high-residual case. It can be observed that the probability of

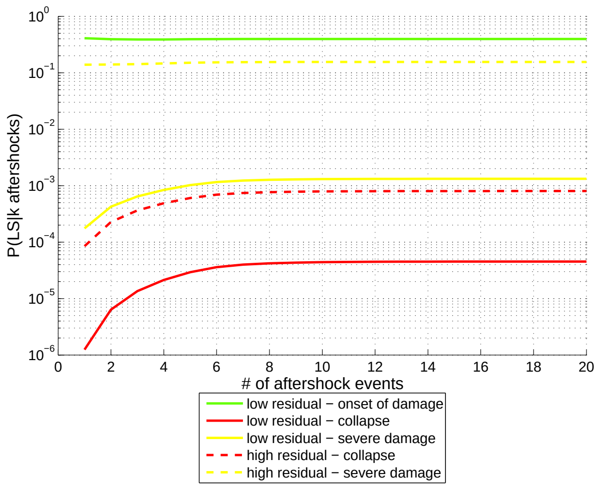

Figure 4: The limit state probabilities given k after-shocks have taken place

exceeding each limit state increases as a function of the first few aftershock events and quickly saturates afterwards. This is because, after a certain number of after-shocks have taken place, the probability of failure given spectral acceleration reaches unity. For the limit state of onset of damage, the low-residual structure reaches the limit state threshold with the occurrence of the first aftershock event.

The time-dependent limit state probabilities are calculated based on the procedure described in Section 2.2 for $T_{max} = 365$ assuming that the repair time for each limit state is much larger than the after-shock inter-arrival times. The results are plotted in Figure 5 for both cases. The same

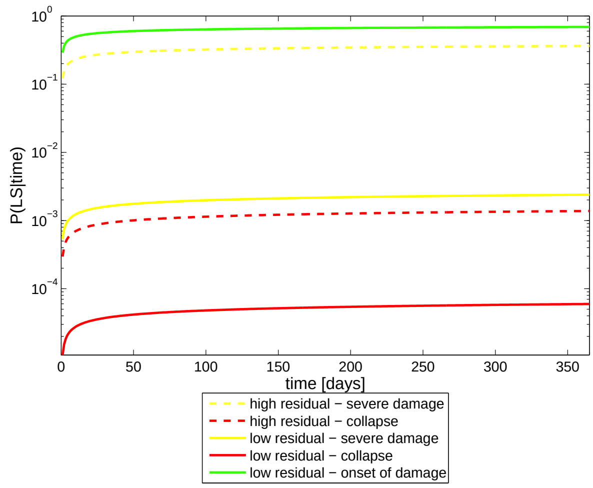

Figure 5: The limit state probabilities during a year elapsed after the main-shock

as in Figure 4, it can be observed that the limit state probability rapidly increases with time and remains constant afterwards. This is caused by the combined effect of the time-decaying rate of after-shocks and the quick saturation of the limit state probabilities as a function of the number of aftershocks.

3.5 *The probability of failure in a 24-hour time interval*

The probability of exceeding the limit state of collapse in a day (24 hours) has been calculated from Equation 17 setting $\Delta T = 1$. The results are plotted in Figure 6 where they are compared against an acceptable mean daily collapse rate of $2 \times 10^{-3}/365$, as a proxy for life safety considerations. This threshold value is on average equivalent to an acceptable mean annual rate of collapse equal to 2×10^{-3}. This verification is done for ensuring life safety for the building occupants. It can be observed that the low-residual structure is immediately below the acceptable threshold for life-safety limit state; whereas, the high-residual case does not verify the acceptable threshold up to around 35 days elapsed after the occurrence of the main-shock. After 35 days, due to the decreasing rate of occurrence of after-shocks, the structure verifies against the life-safety limit state threshold. It should be noted that such a time-variant

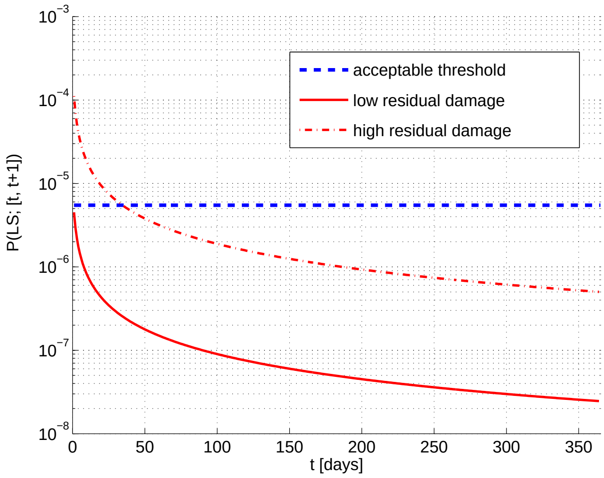

Figure 6: Probability of exceeding the collapse limit state in a day

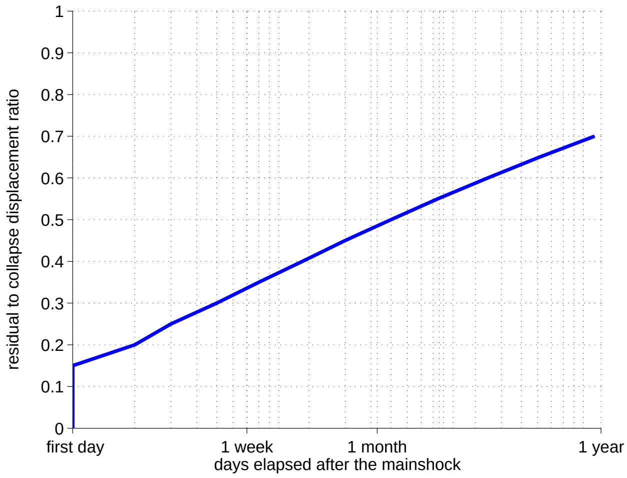

Figure 7: Time elapsed after the occurrence of the main-shock in order to verify the life-safety requirements

performance assessment can be potentially useful for evaluation of the re-occupancy risk for the structure after a certain amount of time has passed from the occurrence of the main shock. In fact, the necessary time elapsed after the occurrence of main-shock in order for the structure to verify the life-safety limit state is calculated for a range of residual to collapse displacement capacity ratios. Figure 7 illustrates the time required in order to verify the collapse limit state for different residual percentiles. It can be observed that the structure immediately verifies the life-safety limit state when the residual damage is minimal; whereas, it might take more than a year before the structure verifies in cases where the residual damage is very significant.

4 CONCLUSIONS

This paper presents a preliminary effort for quantification of the time-variant probability of exceeding various discrete limit states for a structure in an after-shock prone environment. A simple methodology is presented for calculating the probability of exceeding a limit state in a given interval of time elapsed after the occurrence of the main-shock event. This procedure employs a generic after-shock sequence in order to model the time-decay in the mean daily rate of the occurrence of significant after-shocks. The seismic after-shock hazard at the site of the structure is calculated by setting the main-shock moment magnitude as the upper limit for magnitude and is updated using the Bayes formula given that the small-amplitude spectral acceleration of the main-shock at the fundamental period of the structure is known. The progressive damage caused by the sequence of after-shock events is modeled in the form of a suite of different ground motion recordings that are applied (repeatedly) to the simplified structural model. Conditioned on the occurrence of a given number of after-shocks, the statistics of the structural response to the suite of records can be used to calculate the probability of exceeding the limit state capacity. The numerical results are presented for two cases where the structure has undergone low residual damages and high residual damages after the main-shock. It can be observed that the probability of exceeding the limit state capacity increases as a function of the number of significant after-shocks until it reaches a plateau and remains constant afterwards. Conditioned on the occurrence of a given main shock event, the probability of exceeding the limit states of *onset of damage*, *severe damage* and *collapse* in a given interval of time are calculated. It can be observed that the limit state probabilities increase as a function of time although they seem to reach a constant threshold at the end of a year passed from the occurrence of the main-shock. In order to better observe this effect, the collapse limit state probability in a 24-hour period is calculated as the increment of the time-variant limit state probability in a given interval of time (measured in days). In fact, comparing the time-variant probability of collapse in a 24-hour period of time against an acceptable threshold, it can be observed that the strongly damaged structure could be occupied after a certain amount of days has elapsed after the occurrence of the main-shock while the lightly damaged structure could be occupied immediately. This type of verification can be useful for evaluation of re-occupancy risk for the structures located in a zone prone to after-shocks, based on the life-safety criterion. In fact, the necessary time elapsed after the main-shock for the structure to verify the life-safety requirements is calculated as a function of different values of residual to collapse displacement capacity ratio. It is observed that time needed to verify against the life-safety limit state increases exponentially as a function of the level of residual damage undergone after the main-shock. The methodology presented in this work is adaptive in the sense that the limit state probability evaluations can be updated in time as more after-shock events take place. Finally, the proposed methodology could be used for post-earthquake decision-making between a set of viable actions such as, evacuation, shut-down, repair and re-occupancy.

5 ACKNOWLEDGEMENTS

The authors would like to acknowledge Carmine Galasso for his kind help in organizing and sorting the acceleration time-histories. This work was supported by MAMAS Project funded by Ministero dell'Istruzione, dell'Università e della Ricerca (MIUR). This support is gratefully acknowledged. Any opinions, findings and conclusions or recommendations expressed in this material are those of the authors and do not necessarily reflect those of the sponsors.

References

Asprone D, Jalayer F, Prota A, Manfredi G. Probabilistic assessment of blast-induced progressive collapse in a seismic retrofitted RC structure. *Proceeding of the 14th World Conference on Earthquake Engineering*, Beijing, October, 2008.

Mander JB, Priestley JN, Park R. Theoretical Stress-Strain Model for Confined Concrete. *Journal of Structural Engineering.* **114**(8), pp. 1804-1826, 1988.

Meletti C., Valensise G. Zonazione Sismogenetica ZS9. *Instituto Nazionale di Geofisica e Vulcanologia*, Marzo 2004.

Reasenberg P., Jones L. Earthquake hazard after a main-shock in California. *Science*, **243**:11731175, 1989.

Yeo G, Cornell CA. Post-quake decision analysis using dynamic programming. *Earthquake Engineering and Structural Dynamics.* **38**(1):79-93 January 2009.

Yeo G, Cornell CA. Equivalent constant rates for post-quake seismic decision making. *Structural Safety.* early view, January 2009.

Sabetta F., Pugliese A. Estimation of response spectra and simulation of nonstationary earthquake ground motions. *Bulletin of the Seismological Society of America*, **86**(2):337-352, 1996.